



Angiopoietin-like 3 regulates hepatocyte proliferation and lipid metabolism in zebrafish



So-Hyun Lee^{a,b}, Ju-Hoon So^b, Hyun-Taek Kim^b, Jung-Hwa Choi^b, Mi-Sun Lee^b,
Seok-Yong Choi^{c,d}, Cheol-Hee Kim^{b,*,1}, Min Jung Kim^{a,*,1}

^a Department of Biological Sciences, Sookmyung Women's University, Seoul, Republic of Korea

^b Department of Biology, Chungnam National University, Daejeon, Republic of Korea

^c Department of Biomedical Sciences, Chonnam National University Medical School, Gwangju, Republic of Korea

^d School of Biological Sciences and Technology, Chonnam National University, Gwangju, Republic of Korea

ARTICLE INFO

Article history:

Received 5 March 2014

Available online 28 March 2014

Keywords:

Angiopoietin-like 3

Angptl3

Zebrafish

Liver

Hypobetalipoproteinemia

Angiogenesis

ABSTRACT

Loss-of-function mutations in angiopoietin-like 3 (ANGPTL3) cause familial hypobetalipoproteinemia type 2 (FHBL2) in humans. ANGPTL3 belongs to the angiopoietin-like family, the vascular endothelial growth factor family that is structurally similar to angiopoietins and is known for a regulator of lipid and glucose metabolism, although it is unclear how mutations in ANGPTL3 lead to defect in liver development in the vertebrates. We report here that *angptl3* is primarily expressed in the zebrafish developing liver and that morpholino (MO) knockdown of *Angptl3* reduces the size of the developing liver, which is caused by suppression of cell proliferation, but not by enhancement of apoptosis. However, MO knockdown of *Angptl3* did not alter angiogenesis in the developing liver. Additionally, disruption of zebrafish *Angptl3* elicits the hypocholesterolemia phenotype that is characteristic of FHBL2 in humans. Together, our findings propose a novel role for *Angptl3* in liver cell proliferation and maintenance during zebrafish embryogenesis. Finally, *angptl3* morphants will serve as a good model for understanding the pathophysiology of FHBL2.

© 2014 Elsevier Inc. All rights reserved.

1. Introduction

Hypobetalipoproteinemia (HBL) is a lipoprotein metabolism disorder featuring permanently low levels (below the 5th percentile) of apolipoprotein B (apoB), total cholesterol, and low-density lipoprotein (LDL) cholesterol. HBL is a relatively common disorder, but usually asymptomatic [1]. The genetic causes of HBL have been identified to be mutations of microsomal triglyceride transfer protein [2], apolipoprotein B (ApoB) [3], and ATP-binding cassette transporter [4]. In addition, loss of function mutations in the angiopoietin-like 3 protein (ANGPTL3) was reported to be associated with HBL [5].

Conklin and colleagues cloned human and mouse ANGPTL3 (460 and 455 amino acids, respectively), and showed that ANGPTL3 is specifically expressed in the liver, with minor

expression in the kidney. They also demonstrated that during mouse embryonic development, ANGPTL3 starts to be expressed at embryonic day 15 [6]. Several reports have uncovered a number of functions of ANGPTL3. First, ANGPTL3 suppresses lipoprotein lipase activity [7] and disruption of ANGPTL3 in mice alters lipid metabolism [1,5,8]. Moreover, a defect in human ANGPTL3 elicits familial hypobetalipoproteinemia type 2 (FHBL2) [9]. Second, ANGPTL3 binds to $\alpha_v\beta_3$ integrin, thereby stimulating endothelial cell adhesion and migration, leading to the induction of angiogenesis [10]. Third, ANGPTL3 is involved in the control of motility and permeability of podocytes [11]. Fourth, ANGPTL3 stimulates expansion of hematopoietic stem cells (HSCs) [12] and maintains the stemness of HSCs in the bone marrow niche [13].

Although *Angptl3* is expressed during embryonic development in mice, little is known regarding its role in vertebrate development [6]. Zebrafish is a good model organism to study vertebrate development, and the homology between zebrafish and human ANGPTL3 protein is very high in amino acid sequence [14], suggesting that zebrafish and mammalian ANGPTL3 may play a comparable role in development. Thus, we set out to determine a role for *Angptl3* in zebrafish embryonic development.

* Corresponding authors. Fax: +82 42 822 9690 (C.-H. Kim), +82 2 2077 7322 (M.J. Kim).

E-mail addresses: zebrakim@cnu.ac.kr (C.-H. Kim), minkim@sookmyung.ac.kr (M.J. Kim).

¹ These authors contributed equally to this work and are co-corresponding authors.

2. Materials and methods

2.1. Zebrafish maintenance

Wild type zebrafish (TL and AB* strain) and *Tg(flk1:egfp)⁸⁴³* line [15] were maintained at 28.5 °C using standard procedures [16] and staged in hours post-fertilization (hpf) or days post-fertilization (dpf) as per standard criteria [17]. Embryos were treated with 1-phenyl-2-thiourea (Sigma–Aldrich, USA) to suppress melanin synthesis.

2.2. Isolation of full-length *angptl3*, RT-PCR and whole mount in situ hybridization

Zebrafish *angptl3* was amplified from the cDNA by PCR using forward (5'-CGA TCC CAG ACT GAA GCA GTG AGC AA-3') and reverse (5'-CTA GGG TCA GGG ATT ATT GAA AT-3') primers, and then cloned into the pCS2+ or pCS2+ -EGFP (enhanced green fluorescent protein) vector. Expression levels of *angptl3* in the zebrafish embryos at indicated stages were assessed by RT-PCR from the cDNA with specific *angptl3* forward (5'-GCA TCT TCC AGA AGC TCA ACG TC-3') and reverse (5'-TCC AAC GTG AAG GTG TAC TCG-3') primers. The *angptl3* riboprobes were generated with a DIG RNA Labeling Kit (Roche, Germany). In situ hybridization was performed with standard protocols [18]. The resulting images were taken by an MZ-16 stereomicroscope (Leica, Germany), and then assembled using Adobe Photoshop CS3.

2.3. Microinjection of embryos with *angptl3* morpholinos and mRNA

The *angptl3* mRNA was in vitro transcribed using a SP6 mMES-SAGE mMACHINE kit (Ambion, USA). Morpholino oligonucleotides (MO) (5'-TAG CCA CAA AAG CAG GAT CAA CAT C-3'; Gene-Tools, USA) were used to target the translation start codon and part of the 5'-UTR of the *angptl3* mRNA. The *angptl3* MO (2.2 ng) or/and *angptl3* mRNA (32 pg) were sequentially injected into one-cell stage embryos. The injected embryos were incubated until the indicated stage and then analyzed by whole mount in situ RNA hybridization.

2.4. Staining of embryos with CY3-SA

To specifically stain the liver and gut of zebrafish larvae, embryos at 4 dpf were stained with CY3-SA (1:500, Sigma–Aldrich) as described previously [19] and imaged with a Zeiss confocal laser scanning microscope (LSM5, Zeiss, Germany).

2.5. Detection of cell proliferation and apoptosis

Embryos at 5 dpf were injected with BrdU and were fixed 2 h after injection. Embryos were stained with a 5-bromo-2'-deoxyuridine antibody (BrdU; Sigma–Aldrich) and BrdU incorporated cells were detected by immunocytochemistry. For detection of apoptotic cells, embryos were subjected to TUNEL assay using an In Situ Cell Death Detection Kit (Roche), embedded in OCT medium (Tissue-Tek, Japan), and cryosectioned to 10 µm in thickness.

2.6. Lipid staining

2.6.1. Oil red O

Zebrafish embryos were fixed with 4% paraformaldehyde in phosphate buffer and stained with a filtered Oil red O (Sigma–Aldrich). Images were captured with a MZ-16 stereomicroscope (Leica).

2.6.2. 7-Nitrobenz-2-oxa-1,3-diazol-4-yl(NBD)-cholesterol

Zebrafish larvae were labeled with NBD-cholesterol as described previously [20] and imaged under a Zeiss Axiocam 2 mounted on a MZ FLIII (Leica). For statistical analysis, intestinal fluorescence was scored on a 3-point scale (weak, moderate, and bright) and *p* value was obtained by Student's *t*-test.

3. Results

3.1. *angptl3* mRNA is expressed in the developing zebrafish liver

Zebrafish Angptl3 protein (NCBI accession number NP_571893.1) [14] is very similar in amino acid sequence to the mouse (NP_038941.1; 46.5% identity and 67.8% similarity) and human (NP_055310.1; 44.4% identity and 65.7% similarity) counterparts. To determine the temporal expression pattern of *angptl3* mRNA, we carried out RT-PCR analysis with *angptl3* specific primers. *angptl3* mRNA was not maternally expressed, but expressed from 48 hpf onward (Fig. 1A). We performed in situ RNA hybridization on zebrafish larvae with *angptl3* riboprobes to determine the spatial expression pattern. Consistent with a previous report [14], *angptl3* was weakly expressed in the yolk syncytial layer and ventral regions of yolk ball (data not shown) at early stage of embryogenesis. Expression of *angptl3* was predominantly detected in the liver from 38 hpf onward, at which stage furrow develops between the liver bud and the esophagus (Fig. 1B–E, B'–D') [21], while *angptl3* was not detected in the pancreas rudiment at all stages. Transverse sections of the embryos at 5 dpf confirmed the liver-specific expression of *angptl3* (Fig. 1E'), consistent with the liver-specific expression of *angptl3* in adult human and mouse [6].

3.2. *Angptl3* is not involved in vasculogenesis and angiogenesis in zebrafish larvae

To study a role for Angptl3 in zebrafish development, we designed MO targeting the translation start site of *angptl3* (referred to as *angptl3* MO hereafter). To confirm the knockdown efficiency of *angptl3* MO, we generated construct encoding the *angptl3* 3' untranslated region (UTR) fused to EGFP and synthesized *angptl3-egfp* mRNA. We co-microinjected *angptl3* MO and *angptl3-egfp* mRNA into one-cell stage embryos. The *angptl3* MO almost completely abolished the expression of *angptl3-EGFP* (Fig. 2A), verifying the knockdown efficiency of the MO.

As human and mouse ANGPTL3 were reported to be implicated in angiogenesis [10], we sought to monitor whether *angptl3* is involved in angiogenesis in zebrafish larvae. To this end, we microinjected the *angptl3* MO into one-cell stage *Tg(flk1:egfp)⁸⁴³* embryos that express EGFP in the vascular system [15]. In the *angptl3* MO injected *Tg(flk1:egfp)⁸⁴³* embryos at 4 dpf, decrease in the size of liver was noted (Fig. 2B, upper panel). However, no significant difference was observed in the overall vessel formation between the *angptl3* morphants and control embryos (Fig. 2B, lower panel). These results suggest that *angptl3* is not involved in vasculogenesis and angiogenesis in zebrafish development. Rather, it is involved in the liver development.

3.3. *Angptl3* is required for liver development, but not pancreas and gut formation

The *angptl3* morphants stayed alive and no gross morphological phenotype was detected. As *angptl3* expression is limited to the liver during zebrafish development, we studied a role for Angptl3 in embryonic liver development by whole mount in situ RNA hybridization on *angptl3* morphants with various liver marker

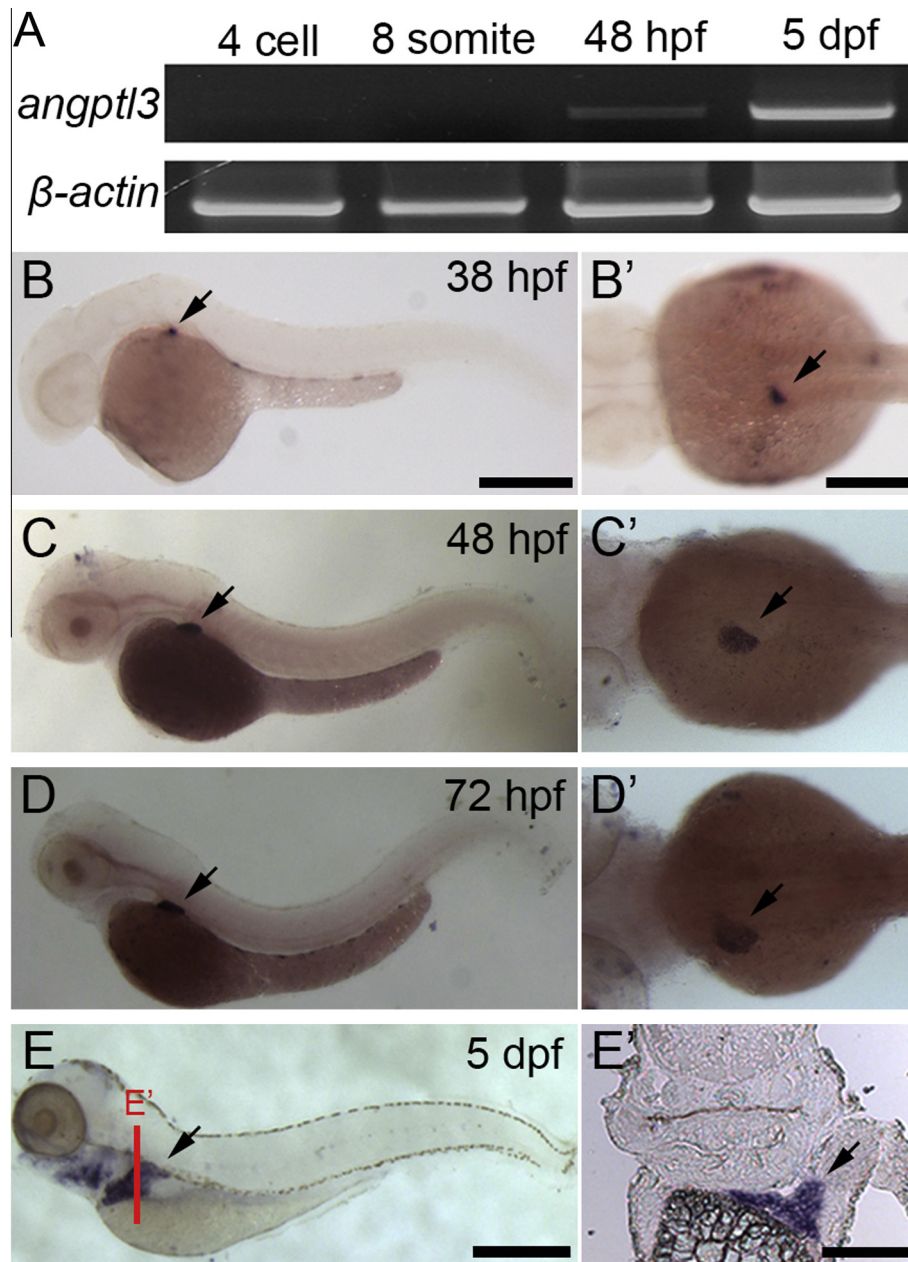


Fig. 1. Zebrafish *angptl3* in the embryonic liver. (A) Zebrafish RNA was extracted from zebrafish embryos at the indicated stages, and amplified by RT-PCR with *angptl3* or β -actin primers. β -Actin was used as a loading control. (B–E) Whole mount in situ RNA hybridization with *angptl3* riboprobes. Lateral views anterior to the left. (B', C', D') The same embryos in B, C, and D, respectively, dorsal views anterior to the left. (E') A cross-section of the embryo in E at the level indicated by the line in E. The arrows indicate the livers. Scale bars represent 250 μ m (B, E) or 100 μ m (B').

riboprobes. Expression of *cyp2j22* was not altered in liver at 2 dpf (Fig. 2C). In *angptl3* morphants at 3 dpf, however, expression of liver markers (*cyp2j22* and *foxa3*) was reduced compared to control embryos (Fig. 2C) and this reduction became more pronounced with developmental time (data not shown). Of note, the size of the pancreas and gut was unaltered in *angptl3* morphants at 3 dpf, as demonstrated by in situ RNA hybridization with *foxa3* riboprobes (Fig. 2C), a marker for liver, pancreas and gut, suggestive of a liver-specific role for *angptl3*. To confirm these findings, we stained control and *angptl3* morphant embryos at 4 dpf with CY3-SA, a dye specific for epithelium structure of liver and gut, and observed reduction in liver size, but not gut size (Fig. 2C). Collectively, these findings suggest that *angptl3* is involved in the

development of liver at later stages, but not in the initiation of liver development.

3.4. The *angptl3* mRNA can rescue a small liver phenotype in *angptl3* morphants

We performed a rescue experiment to verify the specificity of a small liver phenotype in *angptl3* morphants. In situ RNA hybridization with *fabp10* riboprobes, a liver marker, revealed that the area of *fabp10* expression was markedly decreased in *angptl3* morphants at 3 dpf and returned to the almost normal size by co-injection of *angptl3* mRNA and MO (Fig. 2D, D'). These findings

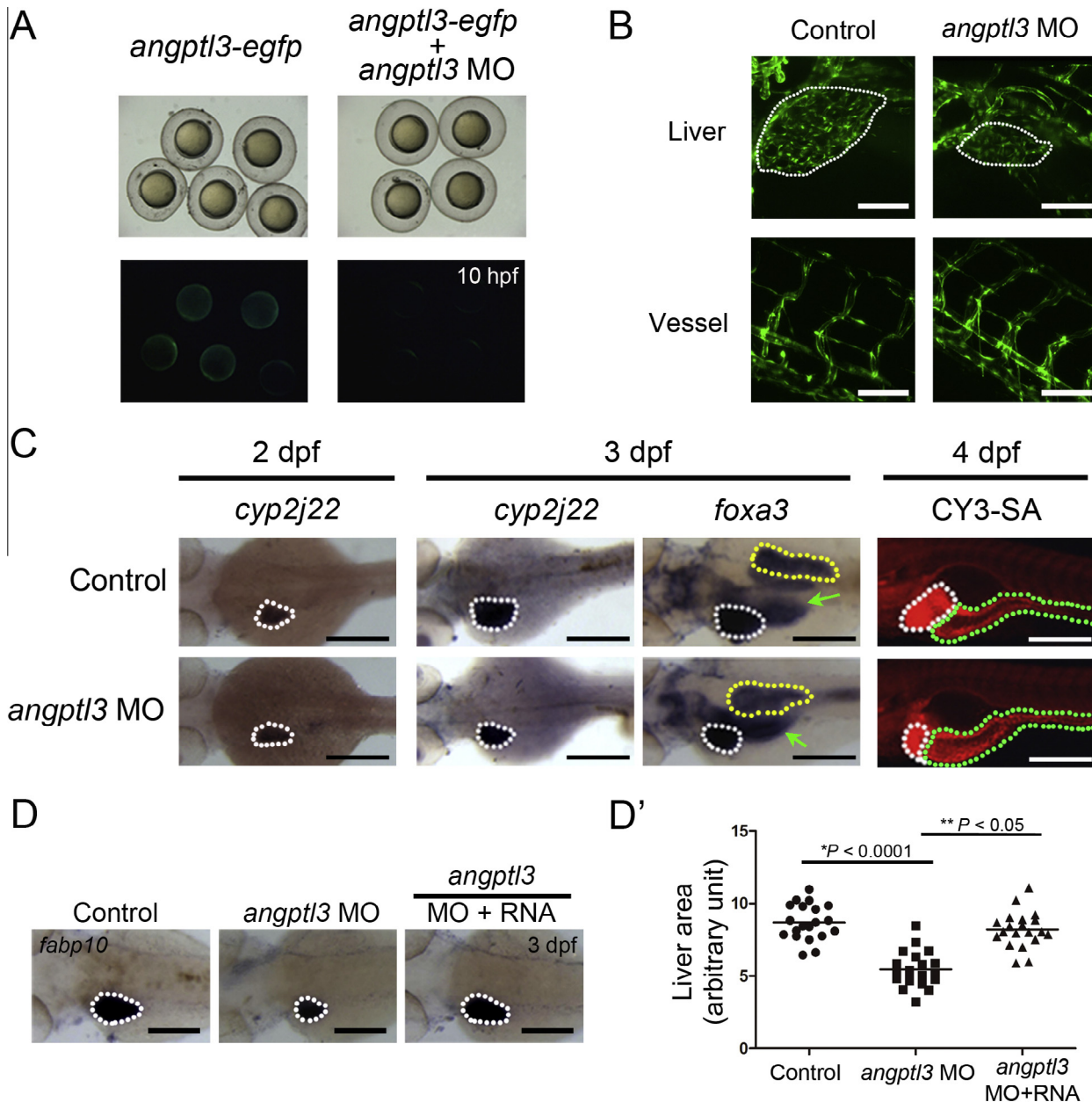


Fig. 2. Morpholino knockdown of *angptl3* affects the size of the developing liver, not the vessel formation. (A) Zebrafish embryos injected with mRNA encoding *angptl3* fused to *egfp* alone or in combination with *angptl3* MO, imaged by either transmitted (upper) or fluorescence (lower) stereomicroscopy. (B) *Tg(flk1:egfp)^{s843}* embryos were injected with control MO or *angptl3* MO, and imaged with a fluorescence stereomicroscope at 4 dpf. The upper panel shows the liver area and the lower panel, the trunk area. Lateral views anterior to the left. Scale bar = 50 μ m. (C) Zebrafish embryos injected with *angptl3* MO were subjected to whole mount in situ RNA hybridization with the *cyp2j22* or *foxa3* riboprobes (left three panels; dorsal views anterior to the left), or stained with CY3-SA, a dye specific for liver and gut (rightmost panel; lateral views anterior to the left). The *cyp2j22* is a liver-specific marker and *foxa3*, a marker for liver, pancreas and gut. White dotted circles indicate the liver; yellow dotted circles, pancreas; green arrow and green dotted circle, gut. Scale bar = 100 μ m. (D) Rescue of *angptl3* MO phenotype with *angptl3* mRNA in the developing liver. *angptl3* mRNA or *angptl3* mRNA/MO were injected into one-cell stage zebrafish embryos and then processed at 6 dpf for whole mount in situ RNA hybridization with *fabp10* riboprobes. Scale bar = 100 μ m. (D') Liver size of embryos stained with *fabp10* riboprobes shown in (D) was quantified using the Image J software. The p value was determined by the two-tailed homoscedastic Student's t -test ($n = 14, 10$, and 6 [control, *angptl3* MO, and *angptl3* MO plus *angptl3* RNA, respectively]). * $p < 0.0001$; ** $p < 0.05$. (For interpretation of the references to color in this figure legend, the reader is referred to the web version of this article.)

demonstrate that a small liver phenotype in *angptl3* morphants is indeed caused by downregulation of *angptl3*.

3.5. *Angptl3* suppresses cell proliferation in the developing zebrafish liver

To understand the decreased size of liver in *angptl3* morphants, we assessed apoptosis in the *angptl3* morphants. TUNEL assay

revealed no significant difference in the liver between control and *angptl3* morphant larvae (data not shown). We next performed BrdU labeling to examine cell proliferation in the liver of control and *angptl3* morphant larvae at 5 dpf. A significant decrease in the number of BrdU⁺ cells was detected in the liver of 5-dpf *angptl3* morphants compared to that in the control liver (Fig. 3), whereas no change in the number of BrdU⁺ cells was detected in a control tissue (the eyes) between the morphants and control larvae

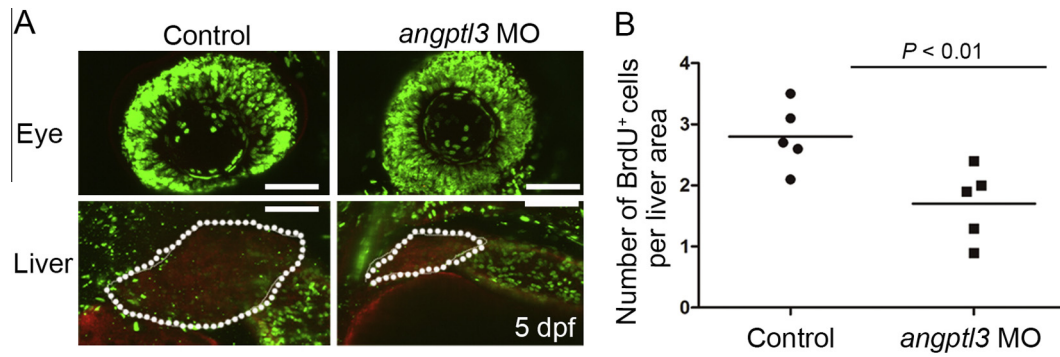


Fig. 3. Knockdown of Angptl3 suppresses cell proliferation in the developing liver. (A) Zebrafish embryos were injected with control MO or *angptl3* MO, raised to 5 dpf, stained with CY3-SA, a dye specific for liver and gut, co-labeled with BrdU, and imaged by fluorescence stereomicroscope. CY3-SA is shown in red and BrdU⁺ cells, in green. Dotted circles outline the livers. Lateral views anterior to the left are shown. Scale bar = 50 μm. (B) BrdU⁺ cells in the liver shown in (A) were scored. The *p* value was determined by the two-tailed homoscedastic Student's *t*-test (*n* = 3 and 5 [control and *angptl3* MO, respectively]). *p* < 0.01. (For interpretation of the references to color in this figure legend, the reader is referred to the web version of this article.)

(Fig. 3A, upper panel). These results indicate that *angptl3* is involved in the regulation of cell proliferation, but not apoptosis, in the developing liver.

3.6. *angptl3* morphants display FHBL2 phenotype

Since loss-of function mutations in ANGPTL3 cause FHBL2 in humans, we sought to check if *angptl3* knockdown decreases lipid droplet accumulation *in vivo*. To this end, we first assessed lipid metabolism in live *angptl3* morphants by feeding the fluorescent cholesterol analog, NBD-cholesterol. *angptl3* morphants failed to concentrate NBD-cholesterol in the gall bladders (GB), in contrast to the concentrated NBD-cholesterol in the GB in control zebrafish larvae (Fig. 4A), suggesting that *angptl3* morphants have a defect in the trafficking of sterol-like molecules.

Next, we stained *angptl3* morphants with Oil red O to assess the effect of *angptl3* knockdown on lipid absorption. In the morphants at 6 dpf, the extent of overall Oil red O staining, readout of

triglyceride levels, was decreased compared to control larvae (Fig. 4B). *angptl3* morphants exhibited decreased yolk consumption and absorption of dietary neutral lipids, and showed a near absence of hepatic and intestinal lipid droplet staining (Fig. 4B–B'). Moreover, although vessel formation was normal (Fig. 2B), Oil red O staining for vessel in the trunk was significantly decreased in *angptl3* morphant (Fig. 4B''). Taken together, these findings show that *angptl3* morphants mimic the hypocholesterolemic phenotypes of FHBL2, a marked reduction of all plasma lipids and total cholesterol.

4. Discussion

Here, we show that zebrafish *angptl3* is exclusively expressed in the liver of developing embryos and that knockdown of *angptl3* inhibits cell proliferation in the embryonic liver.

Fujimoto and colleagues reported that the liver weight of ANGPTL3 null mice at 15 weeks of age was comparable to that

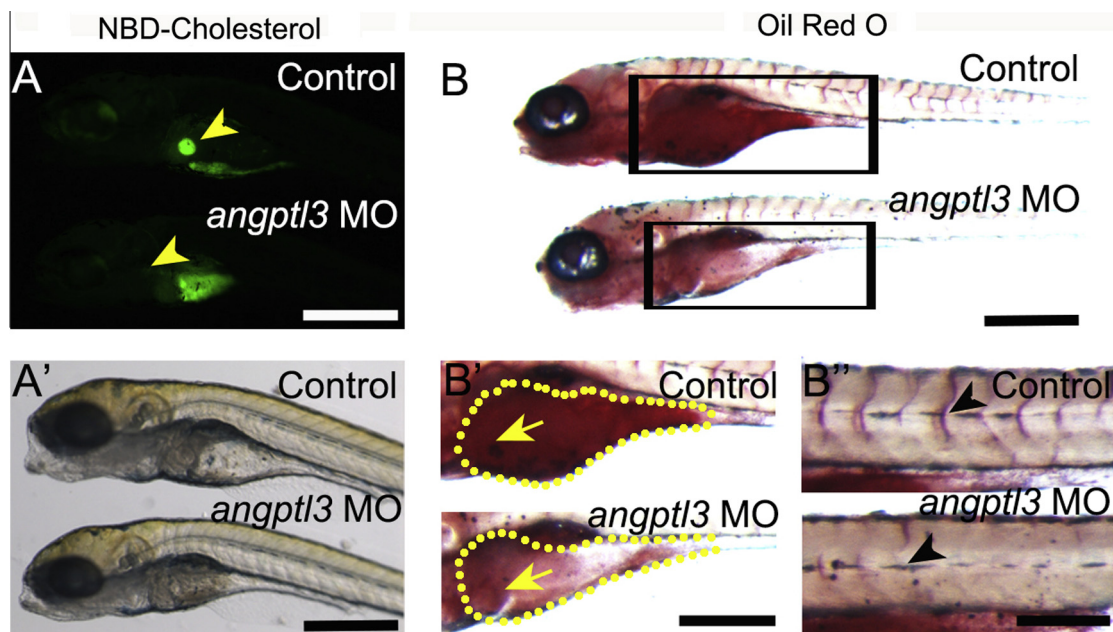


Fig. 4. Knockdown of *angptl3* decrease lipid accumulation in zebrafish liver, intestine and vessels. (A–A') Lateral fluorescent (A) and transmitted views (A') of larvae stained with NBD-cholesterol. Yellow arrowheads in (A) indicate the lipid processing in the gall bladder. The transmitted image of *angptl3* morphants was indistinguishable from control larvae at 6 dpf (A'). (B–B'') Lateral view of larvae at 6 dpf stained with Oil red O. Boxed regions (B) are magnified in (B'). Yellow arrows denote the liver and dotted outlines, yolk and intestine of zebrafish larvae. Black arrowheads indicate the Oil red O staining in the vessels of larvae. Scale bar = 200 μm. (For interpretation of the references to color in this figure legend, the reader is referred to the web version of this article.)

of WT littermates [1], whereas we observed a significant decrease in the liver size of zebrafish *angptl3* morphants compared to that of control embryos. There are two possibilities that might explain this inconsistency between mouse and zebrafish. First, the reduced size of the developing liver in ANGPTL3 null animals may be restored to a normal size in later stages of development by a compensatory mechanism. Unfortunately, we could not currently verify this possibility because there are no reports on the size of the embryonic liver in ANGPTL3 null mice or of the adult liver in *angptl3* null zebrafish. Second, although the zebrafish and mouse ANGPTL3 proteins have very similar amino acid sequences, their roles in liver development may differ.

Is ANGPTL3 involved in angiogenesis in the liver? Gerber and colleagues reported that ANGPTL3 promotes angiogenesis in the rat corneal assay [10]. However, we did not observe any noticeable change in vasculogenesis and angiogenesis in the liver of *angptl3* morphant zebrafish larvae compared to that of control larvae. This discrepancy may reflect differences in the organisms and tissues tested. However, we found that lipid level in the vessel was significantly decreased in the *Angptl3* knockdown embryos.

The phenotype of *angptl3* morphants is reminiscent of the hypocholesterolemia in patients with FHBL2. First, the extent of lipid absorption was low in *angptl3* morphants compared to control larvae. Second, although we found that the vasculogenesis was normal in *angptl3* morphants, the level of lipid deposition in the vessel of *angptl3* morphants was lower than control larvae. Low levels of lipid staining in the vessels of *angptl3* morphants are reminiscent of low arterial stiffness and reduction of serum LDL cholesterol in FHBL patients [22].

What is the molecular mechanism by which knockdown of *Angptl3* suppresses cell proliferation in the developing liver? Lodish and colleagues reported a similar finding that ANGPTL3 stimulates expansion of HSCs [12]. Without identification and characterization of a receptor for ANGPTL3, however, it may not be possible to determine the underlying molecular mechanism. Nevertheless, a recent report from the Broxmeyer lab that the coiled-coil domain of ANGPTL3 promotes phosphorylation of the extracellular signal-regulated kinase, one of the signaling molecules regulating cell proliferation [23], might provide a hint at the involvement of the mitogen-activated protein kinase (MAPK) pathway in the ANGPTL3 regulation of liver development.

Thus, further study on a molecular mechanism by which *Angptl3* regulates proliferation of hepatocytes in the zebrafish system will better our understanding of liver development at molecular levels and provide an animal model system for FHBL2 in humans.

Author contributions

S.C., C.K., and M.J.K. conceived and designed experiments. S.L., J.S., and M.J.K. performed the experiments. S.L., J.S., H.K., J.C., M.L., S.C., C.K., and M.J.K. provided zebrafish lines and analyzed the data. S.L., S.C., and M.J.K. wrote the manuscript.

Competing interest

The authors declare that they have no competing financial interests.

Acknowledgments

We thank Prof. Didier Stainier at UCSF, USA for the *Tg(flk1:egfp)⁸⁴³* line. This research was supported by Basic Science Research Program through the National Research Foundation of Korea (NRF) funded by the Ministry of Education, Science, and Technology (2009-0068388).

References

- [1] K. Fujimoto, R. Koishi, T. Shimizugawa, Y. Ando, *Angptl3*-null mice show low plasma lipid concentrations by enhanced lipoprotein lipase activity, *Exp. Anim.* 55 (2006) 27–34.
- [2] V. Sheena, R. Hertz, I. Berman, J. Nussbeck, J. Bar-Tana, Transcriptional suppression of human microsomal triglyceride transfer protein by hypolipidemic insulin sensitizers, *Biochem. Pharmacol.* 70 (2005) 1548–1559.
- [3] R. Huijgen, B. Sjouke, K. Vis, J.S. de Randamie, J.C. Defesche, J.J. Kastelein, G.K. Hovingh, S.W. Fouchier, Genetic variation in APOB, PCSK9, and ANGPTL3 in carriers of pathogenic autosomal dominant hypercholesterolemic mutations with unexpected low LDL-C levels, *Hum. Mutat.* 33 (2012) 448–455.
- [4] A. Von Eckardstein, C. Langer, T. Engel, I. Schaukal, A. Cignarella, J. Reinhardt, S. Lorkowski, Z. Li, X. Zhou, P. Cullen, G. Assmann, ATP binding cassette transporter ABCA1 modulates the secretion of apolipoprotein E from human monocyte-derived macrophages, *FASEB J.* 15 (2001) 1555–1561.
- [5] R. Koishi, Y. Ando, M. Ono, M. Shimamura, H. Yasuno, T. Fujiwara, H. Horikoshi, H. Furukawa, *Angptl3* regulates lipid metabolism in mice, *Nat. Genet.* 30 (2002) 151–157.
- [6] D. Conklin, D. Gilbertson, D.W. Taft, M.F. Maurer, T.E. Whitmore, D.L. Smith, K.M. Walker, L.H. Chen, S. Wattler, M. Nehls, K.B. Lewis, Identification of a mammalian angiopoietin-related protein expressed specifically in liver, *Genomics* 62 (1999) 477–482.
- [7] T. Shimizugawa, M. Ono, M. Shimamura, K. Yoshida, Y. Ando, R. Koishi, K. Ueda, T. Inaba, H. Minekura, T. Kohama, H. Furukawa, ANGPTL3 decreases very low density lipoprotein triglyceride clearance by inhibition of lipoprotein lipase, *J. Biol. Chem.* 277 (2002) 33742–33748.
- [8] A. Koster, Y.B. Chao, M. Mosior, A. Ford, P.A. Gonzalez-DeWhitt, J.E. Hale, D. Li, Y. Qiu, C.C. Fraser, D.D. Yang, J.G. Heuer, S.R. Jaskunas, P. Eacho, Transgenic angiopoietin-like (*angptl*) 4 overexpression and targeted disruption of *angptl4* and *angptl3*: regulation of triglyceride metabolism, *Endocrinology* 146 (2005) 4943–4950.
- [9] K. Musunuru, J.P. Pirruccello, R. Do, G.M. Peloso, C. Guiducci, C. Sougnez, K.V. Garimella, S. Fisher, J. Abreu, A.J. Barry, T. Fennell, E. Banks, L. Ambrogio, K. Cibulskis, A. Kerynsky, E. Gonzalez, N. Rudzicz, J.C. Engert, M.A. DePristo, M.J. Daly, J.C. Cohen, H.H. Hobbs, D. Altshuler, G. Schonefeld, S.B. Gabriel, P. Yue, S. Kathiresan, Exome sequencing, ANGPTL3 mutations, and familial combined hypolipidemia, *N. Engl. J. Med.* 363 (2010) 2220–2227.
- [10] G. Camenisch, M.T. Pisabarro, D. Sherman, J. Kowalski, M. Nagel, P. Hass, M.H. Xie, A. Gurney, S. Bodary, X.H. Liang, K. Clark, M. Beresini, N. Ferrara, H.P. Gerber, ANGPTL3 stimulates endothelial cell adhesion and migration via integrin α v β 3 and induces blood vessel formation in vivo, *J. Biol. Chem.* 277 (2002) 17281–17290.
- [11] X. Gao, H. Xu, H. Liu, J. Rao, Y. Li, X. Zha, Angiopoietin-like protein 3 regulates the motility and permeability of podocytes by altering nephrin expression in vitro, *Biochem. Biophys. Res. Commun.* 399 (2010) 31–36.
- [12] C.C. Zhang, M. Kaba, G. Ge, K. Xie, W. Tong, C. Hug, H.F. Lodish, Angiopoietin-like proteins stimulate ex vivo expansion of hematopoietic stem cells, *Nat. Med.* 12 (2006) 240–245.
- [13] J. Zheng, H. Huynh, M. Umikawa, R. Silvany, C.C. Zhang, Angiopoietin-like protein 3 supports the activity of hematopoietic stem cells in the bone marrow niche, *Blood* 117 (2011) 470–479.
- [14] V.N. Pham, B.L. Roman, B.M. Weinstein, Isolation and expression analysis of three zebrafish angiopoietin genes, *Dev. Dyn.* 221 (2001) 470–474.
- [15] S.W. Jin, D. Beis, T. Mitchell, J.N. Chen, D.Y. Stainier, Cellular and molecular analyses of vascular tube and lumen formation in zebrafish, *Development* 132 (2005) 5199–5209.
- [16] M. Westerfield, *The Zebrafish Book: A Guide for the Laboratory Use of Zebrafish (Danio rerio)*, fifth ed., University of Oregon Press, 2007.
- [17] C.B. Kimmel, W.W. Ballard, S.R. Kimmel, B. Ullmann, T.F. Schilling, Stages of embryonic development of the zebrafish, *Dev. Dyn.* 203 (1995) 253–310.
- [18] C. Thisse, B. Thisse, High-resolution in situ hybridization to whole-mount zebrafish embryos, *Nat. Protoc.* 3 (2008) 59–69.
- [19] K.C. Sadler, A. Amsterdam, C. Soroka, J. Boyer, N. Hopkins, A genetic screen in zebrafish identifies the mutants *vps18*, *nf2* and *foie gras* as models of liver disease, *Development* 132 (2005) 3561–3572.
- [20] S.A. Farber, M. Pack, S.Y. Ho, I.D. Johnson, D.S. Wagner, R. Dosch, M.C. Mullins, H.S. Hendrickson, E.K. Hendrickson, M.E. Halpern, Genetic analysis of digestive physiology using fluorescent phospholipid reporters, *Science* 292 (2001) 1385–1388.
- [21] H.A. Field, E.A. Ober, T. Roeser, D.Y. Stainier, Formation of the digestive system in zebrafish. I. Liver morphogenesis, *Dev. Biol.* 253 (2003) 279–290.
- [22] R.R. Sankatsing, S.W. Fouchier, S. de Haan, B.A. Hutten, E. de Groot, J.J. Kastelein, E.S. Stroes, Hepatic and cardiovascular consequences of familial hypobetalipoproteinemia, *Arterioscler. Thromb. Vasc. Biol.* 25 (2005) 1979–1984.
- [23] H.E. Broxmeyer, E.F. Srour, S. Cooper, C.T. Wallace, G. Hangoc, B.S. Youn, Angiopoietin-like-2 and -3 act through their coiled-coil domains to enhance survival and replating capacity of human cord blood hematopoietic progenitors, *Blood Cells Mol. Dis.* 48 (2012) 25–29.